
Nara: Learning Network-Aware Resource Allocation Algorithms for Cloud Data Centres

Zacharaya Shabka, Georgios Zervas

Optical Networks Group, University College London
 {zacharaya.shabka18, g.zervas}@ucl.ac.uk

Abstract

Data centres (DCs) underline many prominent future technological trends such as distributed training of large scale machine learning models and internet-of-things based platforms. DCs will soon account for over 3% of global energy demand, so efficient use of DC resources is essential. Robust DC networks (DCNs) are essential to form the large scale systems needed to handle this demand, but can bottleneck how efficiently DC-server resources can be used when servers with insufficient connectivity between them cannot be jointly allocated to a job. However, allocating servers' resources whilst accounting for their inter-connectivity maps to an NP-hard combinatorial optimisation problem, and so is often ignored in DC resource management schemes. We present Nara, a framework based on reinforcement learning (RL) and graph neural networks (GNN) to learn network-aware allocation policies that increase the number of requests allocated over time compared to previous methods. Unique to our solution is the use of a GNN to generate representations of server-nodes in the DCN, which are then interpreted as actions by a RL policy-network which chooses from which servers resources will be allocated to incoming requests. Nara is agnostic to the topology size and shape and is trained end-to-end. The method can accept up to 33% more requests than the best baseline when deployed on DCNs with up to the order of $10\times$ more compute nodes than the DCN seen during training and is able to maintain its policy's performance on DCNs with the order of $100\times$ more servers than seen during training. It also generalises to unseen DCN topologies with varied network structure and unseen request distributions without re-training.

1 Introduction

Data center power consumption has roughly doubled every year since 2012 and is expected to account for 3% of global energy requirements, and 20% of global electricity requirements by 2025 [1, 2]. Servers alone account for roughly 50% of this requirement. Furthermore, servers can use up to 30-40% of their maximum power requirements while idle [3]. Therefore, it is highly desirable to find ways of using server resources more efficiently so that DC's workloads can be fulfilled with less servers. The inability to reliably provision bandwidth guarantees, as well as compute resources within allocations, can compromise packing efficiency and also application performance [4, 5]. Trends in Cloud computing use cases, such as virtualisation or the training of large scale ML models or high performance computing are compute and data intensive and increasingly distributed over multiple servers and require high network capacity and good network guarantees [6, 7, 8]. Disparate growth between compute node performance and node communication bandwidth over the last 18 years ($64\times$ vs $4.8\times$) imposes unwanted locality constraints that negatively affect performance [9]. Competition for this bandwidth is detrimental to job resource provisioning and performance [10]. For this reason, it is desirable to be able to jointly allocate both compute and network resources in a DC to tasks in a

way that has good guarantees for the network resources needed and minimises the congestion imposed in the DCN, which can be detrimental to other applications and resource efficiency in general.

Typically DCs are clustered, where groups of servers are connected within a cluster by high bandwidth networking equipment and simple packing heuristics are used to allocate resources from servers to requests, black-boxing the network within this high-bandwidth region [11, 12]. However, in order to have the highest possible bandwidth in a cluster, state-of-the-art (SotA) networking equipment is required to provide the highest bandwidth-per-port. Such equipment is available from typically only a few vendors, and only available with low port density (number of ports at that bandwidth per switch), resulting in an economic limitation to scaling the network, as well as a compromise between available intra- and inter- cluster connectivity leading to fundamental packing inefficiencies [13, 11, 10]. However, accounting for the network explicitly whilst allocating compute resources across nodes (i.e. network-aware resource allocation) has been shown to map to the ‘Quadratic Assignment Problem’ (QAP) [14], a known NP-Hard combinatorial optimisation (CO) problem. This problem can not be solved exactly for systems of the scale of DCs (≥ 1000 nodes) and will otherwise rely on solutions drawn from hand-designed heuristics which require much domain expertise, and are often limited in the diversity of scenarios they perform well in.

In this work we present Nara, a framework based on policy-gradient reinforcement learning (RL) and graph neural networks (GNN) that can automatically learn effective and novel network-aware packing policies. Nara is demonstrated to be able to generalise to different DCN topologies (with respect to both scale, and shape) and also across multiple distributions of requests with different requirement characteristics, without the need to be re-trained. The GNN produces representations of the available actions (servers that can be allocated to a request), which are used by the policy network to make network-aware allocation decisions. The GNN and policy network are trained end-to-end. We also attempt to infer the basic properties of Nara’s policy by visualising its decisions.

When rolled out on DCN topologies with $10\times$ more servers than the topology seen during training, Nara is able to successfully allocate up to 33% more requests than the best performing baseline heuristic. The policy is also maintained when applied to graphs with $100\times$ more servers than seen during training, and performs well on unseen topologies and request distributions compared to Nara when trained directly on those topologies and distributions.

2 Related Work

The need for network-aware resource allocation in DCs was first shown in [14], where the problem is mapped to the NP-Hard QAP. They provide an offline (i.e. when all requests are known ahead of time) cluster-and-cut based heuristic for solving the problem and show an improvement over random allocation. A min-cost-flow based method mapping compute and network resources to virtual machine (VM) requests is proposed in [15], though the method is not compared against other heuristics and only applies in the offline case. A offline heuristic for solving the graph embedding problem is proposed as a method for co-allocating compute and network resources in [16]. Broad limitations of these aforementioned methods is that they are limited to the offline scenario, where real allocation scenarios exist in the online form of the problem. A method proposed in [17] that operates in a online setting based on bipartite-graphs and breadth first search (BFS) and shows an improvement over random allocation, but can only handle requests with a single resource, and operates on a small (24 node) full bisection-bandwidth network. In the context of resource-disaggregated DCN architectures, [18] proposes an online and network-aware multi-resource allocation method which augments the BFS procedure with bandwidth weighting, and uses a weighted k-shortest paths procedure to ensure connectivity between nodes, which searches through the DCN topology until sufficient resources are provisioned with a preference for locality and bandwidth availability, showing improvement over best-fit and first-fit heuristics. A modified online multi-resource packing method based on cosine similarity which encourages network/locality awareness through a penalty system is introduced in [19]. It is shown to reduce resource fragmentation and increase the number of tasks allocated over a period of time. In our work, we seek to demonstrate a framework that can automatically learn good heuristics to solve the online form of the network-aware DCN multi-resource allocation problem which is robust against changes to the topology, scale and request distribution of the DCN.

A learning architecture using GNNs and RL has been shown in recent years as an effective way to solve canonical graph-based CO problems [20] with a demonstrated ability to not require significant

domain expertise, operate at scale and outperform standard solution methods and other solution frameworks based on different ML architectures such as recurrent neural networks (RNN) [21, 22, 23]. Prior work has been done to solve similar computer-cluster/network related problems using similar methods to those proposed in this work. Computation graph based tasks are scheduled onto compute resources (where the network is not modelled, and compute resources are treated as a simple block of resources) using RL + GNN based methods in [22, 24, 25], showing improvement over previous approaches and a degree of generalisability with respect to the works’ goal of reducing the makespan of a set of jobs which arrive over time. In this work, we model tasks in a simpler way (i.e. without dependency structure) but account explicitly for network structure within the resource pool (i.e. the DCN). Route optimisation and modelling of networks using similar architectures have been demonstrated in [26, 27]. More similar to the problem addressed in this work, [28] solves the virtual network embedding (VNE) problem using GNNs and actor-critic based RL methods and shows improvement over other RL based methods that do not exploit graph structure explicitly. However, the model proposed in this framework cannot be applied to graphs with different scales to those seen during training, and is only demonstrated on graphs with the order of 100 nodes and uniform request distributions. To the best of our knowledge, there has not to date been any work using RL in combination with GNNs to solve the problem of network-aware multi-resource allocation in DCs.

3 Method

3.1 Problem statement

Consider a DCN graph, $G(V, E)$, where each node $v \in V$ is associated with a unique 2-tuple, $\langle c_v, m_v \rangle$, denoting the available CPU and memory resources respectively at that node (i.e. node features). Nodes which represent servers in the DCN have non-zero entries, and nodes representing network switches have zero entries. Similarly, a link $e \in E$ has a 1-tuple denoting its available bandwidth resource $\langle b_e \rangle$ (i.e. link features). A request, r , is denoted as a 4-tuple, $\langle c_r, m_r, b_r, t_r \rangle$ denoting its required compute, memory, bandwidth and holding-period respectively. Requests arrive continuously over time, and their form is not known by the packing entity until they arrive.

In this context, the objective of a resource allocator is to maximise the number of requests that are successfully allocated over time, where a successful allocation consists of a sub-set of nodes $V' \subset V$ that satisfy the following constraints:

1. $\sum_{v \in V'} c_v \geq c_r$
2. $\sum_{v \in V'} m_v \geq m_r$
3. A set of paths, P , can be found between all $v \in V'$ such that $b_e \geq b_r$ for all links $e \in P$

3.2 MDP representation

We restate the problem described above here as a Markov Decision Process (MDP), so that it can be addressed as a RL problem. The DCN environment is event-driven, where an event consists of a new request’s arrival. This means that the ‘time-step’ iterates every time a new request arrives. Requests are received by the packing entity (Nara or heuristic) one at a time and the episode terminates when a pre-specified number of requests has been received. If the packing entity is unsuccessful at allocating a request, that request is dropped and not revisited. Details regarding training parameters and other simulation details are given in Appendices E.3 and G.

State. The state is a 3-tuple, $\langle c_{util}, m_{util}, t_r \rangle$, denoting the current utilization of the compute and memory resources in the DCN (averaged over each server) and the holding-period of the awaiting request, r .

Action. An action consists of choosing a compute/memory node from which some resources will be allocated to the awaiting request. An action is represented as a continuous vector, which is the output of a GNN. This is detailed in Section 3.3.

State Transition. Given a request, r , a set of compute/memory nodes which have already been allocated to r in previous actions, $V_r \subset V$, an action $v \in V, \notin V_r$, and a current time-step, t ; (i) If the

third constraint in 3.1 is violated, de-allocate resources from all $v \in V_r$, drop r and go to the next request; (ii) If the third constraint in 3.1 is not violated, but the resource requirements of r have not yet been satisfied by $\{V_r, v\}$, allocate $\min(v_x, r'_x)$ from v to r , where r' represents the remaining requirements of r given that some resources have already been allocated to it from nodes in V_r and $x \in \{c, m\}$; (iii) If the set of nodes $\{V_r, v\}$ satisfies all of the constraints from 3.1, allocate the networking resources (bandwidth) along the relevant paths (found using a k-shortest paths procedure) and go to the next request; (iv) For the given time-step, de-allocate any previously allocated requests who's holding time has now been satisfied.

Reward. The reward was designed with the following criteria:

1. *The reward signal should incentivise the maximisation of the number of requests served.*
2. *The reward should be independent of the form of the request and it's allocation.* All requests should be treated equally, since the goal is to maximise the number of requests served given an amount of resources in general, not just for requests with certain forms. Similarly, requests of the same size may require resources from a different number of servers at different points throughout the episode as server-resource availability changes, so this should also not affect the reward since it would produce an inconsistent reward signal.
3. *The reward should not be wrapped around a specific DCN metric* (e.g. bandwidth utilisation), since it is not clear from which metric(s) a meaningful reward signal could be derived (e.g. higher/lower bandwidth utilisation does not necessarily mean better avoidance of the network packing bottleneck).

The following form of a request structure was determined as satisfying these properties:

1. x if a request is successfully allocated.
2. y if the most recent action violates the third allocation constraint in section 3.1.
3. z otherwise.

It was found through grid-search (Appendix E.3) that the values for x , y and z of 10, -10 and 0 respectively worked better than other values tested. We note here that if the intermediate reward (i.e. the reward given to server choices that neither complete, nor fail an allocation) z is not zero then the reward signal is coupled to the size/number of servers allocated to a request, which violates the second criteria mentioned above.

3.3 Learning model

We employ a GNN which operates on the DCN graph with the raw node and link features to generate node-embeddings of the servers, and use these embeddings to represent the actions. A policy network then learns to make decisions based on the environment's state and these action representations. Using the GNN to represent actions, rather than concatenating node information in the observation vector [28], allows for the policy-gradient based learning model to scale independently of the size of the DCN topology, enabling it to train and test on topologies of different sizes, similar to the architecture shown in [29]. The parameters of the GNN and policy network are learnt end-to-end using the Proximal Policy Optimisation (PPO) algorithm [30].

3.3.1 Action representation model

We use a GNN based on the GraphSAGE [31] architecture, since it is demonstrated to be able to operate at scale and independently of graph topology. During the message-passing stages, each node v sends to and receives from its neighbours, $N(v)$, a message msg_v consisting of the concatenation of their state representation and the raw feature vector of the edge connecting them. Each node v also modifies their self-representation by concatenating a zero-valued vector of the same size as the raw edge feature vectors to their state so that their shape matches those of the received vectors.

The mailbox is defined as the messages received by node v from neighbouring nodes $v' \in N(v)$ (i.e. $mailbox_v = \{msg_{v'} \mid v' \in N(v)\}$), and we denote $M_v = \{mailbox_v \cup v\}$ as the set containing the self-representation of node v and the received states of all it's neighbours. Associated with the i^{th}

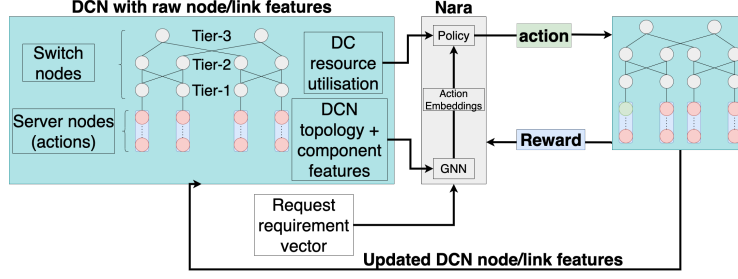


Figure 1: Diagram representing the learning model. Given a request, the action representations are calculated by a GNN using the DCN topology and the raw node and link features of the DCN scaled relative to the requirements of the current request. The policy makes decisions based on these action representations and a DCN state observation vector.

message-passing stage is a NN, W_i . Following this, each node generates a new state representation using a mean-pool based aggregation method as $v = \frac{1}{|N(v)|+1} \sum_{x \in M_v} W_i(x)$. Given a set of nodes that have already been selected to be allocated to the awaiting request, $V' \in V$, the element-wise mean of these representations is concatenated to the representation of each node in the graph, $v \leftarrow [v, \frac{1}{|V'|} \sum_{v \in V'}]$ $\forall v \in V$, so that each action is represented in the context of the actions that have previously been chosen for the awaiting request. Details concerning the implementation of the action representation model are provided in Appendix E.1.

3.3.2 Policy model

The policy consists of two NNs. The first, P_1 , acts directly on the state observation, s , returned by the DCN environment to produce a higher dimensional representation of the observation, $s' = P_1(s)$. Following this, given the representations of each node returned by the action representation model, a second NN P_2 operates on the concatenated vectors $\{[s', v] \forall v \in V\}$ to calculate logits for each node. Action masking is applied after logits have been calculated to nodes with no remaining resources of any type. The policy is stochastic during training, and greedy during rollouts.

4 Experiment

Implementation details of training (training time, tuning etc) is detailed in Appendix E.3.

4.1 Baselines

Random. This is to be used ultimately as a lower bound on performance. Given a request, it will randomly select servers in the DCN until either the request is fully provisioned, or it picks a failing action.

Network Aware Locality Based (NALB). NALB is a network-aware resource allocation algorithm which uses a bandwidth-weighted breadth-first-search algorithm and a bandwidth-weighted k-shortest paths routing algorithm to find suitable nodes and establish connectivity between them respectively [18]. Implementation details regarding the implementation of this are given in Appendix D.2.

Network Unaware Locality Based (NULB). NULB works similarly to the NALB method, except that the breadth-first-search algorithm does not use weighting. Weighting is still used for the k-shortest paths procedure [18]. Implementation details of this are given in Appendix D.2.

Tetris. Tetris is a locality-augmented multi-resource packing heuristic. It uses the cosine similarity between task requirements and server resource availability to calculate scores upon which packing decisions are made. It also imposes a score penalty on non-local resources in order to encourage locality in its decision making [19]. Implementation details are given in Appendix D.1.

4.2 DCN Topology and Generalisability

The topologies used for training and testing are based on the Fabric [13] design principles, which is a 3-tier network design where groups of servers are connected to rack switches (tier-1), rack switches are connected to groups of fabric switches (tier-2) and fabric switches are connected to spine switches (tier-3) as seen in Fig. 1. We term here ‘neighbouring’ racks as those connected to the same set of fabric switches, and non-neighbouring as those connected to different sets of fabric switches. In the context of a DCN environment it is desirable for an allocation method to have some degree of robustness with respect to changing topologies. DCN topologies can in general change dynamically over time (e.g. power outages can render a group of machines temporarily unusable or topology reconfiguration can be implemented by the DCN operator to improve network conditions). Furthermore, DCN request characteristics can change over time and are often difficult to predict, so we incorporate 3 different request distributions and seek to demonstrate firstly that good policies can be learned on each, and secondly that a policy learnt on one generalises well to the others. Four topologies are used, where topology- α is the primary training and testing topology and the rest are described below. More information about the topologies used is given in Appendix F.

Changing the DCN topology shape. Oversubscription between two tiers, n and $n + 1$ of a network refers to the ratio of the maximum amount of information that can flow ‘upwards’ from tier- n into tier- $n + 1$, and how much can flow out of tier- $n + 1$ and into tier- $n + 2$. Topology- β has the same number of server-nodes as topology- α but distributed over twice as many racks with half as many compute/memory nodes per rack. This means that the server-rack oversubscription is halved, and the rack-fabric oversubscription is doubled compared to topology- α . This provides more bandwidth for server-server communication spread over neighbouring racks, but less between non-neighbouring racks.

Changing the DCN topology size. Topology- γ and δ have the same oversubscription properties as topology- α , but are the order of $10\times$ and $100\times$ larger with respect to the number of server-nodes they contain. On topology- γ Nara is compared against the Tetris and random baselines only, since the NALB and NULB methods were prohibitively slow due to their recursive nature. On topology- δ Nara is compared against its performance on the topology seen during training (i.e. to assess how well the policy is preserved at scale) since all baselines (aside from random) were slow to rollout on the larger topology which requires longer episode lengths (more requests) to explore the allocation dynamics of the system since it has significantly more resources.

Changing the data center resource request distribution. In this work, we seek to explore an allocation scenario where the requests arriving at the data center are too large to fit in a single node and so must be distributed. Some real world cluster trace datasets, which detail the requirements of requests arriving at DC clusters over some period of time, are available online. However, in this work we are seeking to explore algorithmic solutions to a widely anticipated problem where requests require more distribution, and have demanding connectivity requirements. To this end, it is necessary to create synthetic datasets on which Nara and the baselines will be tested, since requests of this nature are not characterised on the real-world datasets. However, in order to preserve some realistic properties of the synthetic datasets, we derive two of the three datasets used in this work from two publicly available cluster traces provided by Microsoft Azure [11] and Alibaba [32]. From these datasets, we take the (CPU,Memory) distributions of the requests specified in the traces, scale and bound them to be more demanding on the DC resources (i.e. requiring more servers worth of resources) and pair these values with an increased bandwidth requirement to impose greater demand on the DCN resources. More specific details of how this was done, and how requests were implemented during training and testing is provided in Appendix H. We also generate a third purely synthetic dataset of simple uniform requests.

5 Results

In this work, we focus on two key metrics. Acceptance ratio, $(\frac{\text{Number of accepted requests}}{\text{Number of received requests}})$, indicates how well a packing method is able to avoid the network-imposed bottleneck, since one packing method with higher acceptance ratio than another on the same set of requests on the same DCN topology is able to allocate more requests with the same amount of compute and network resources than the

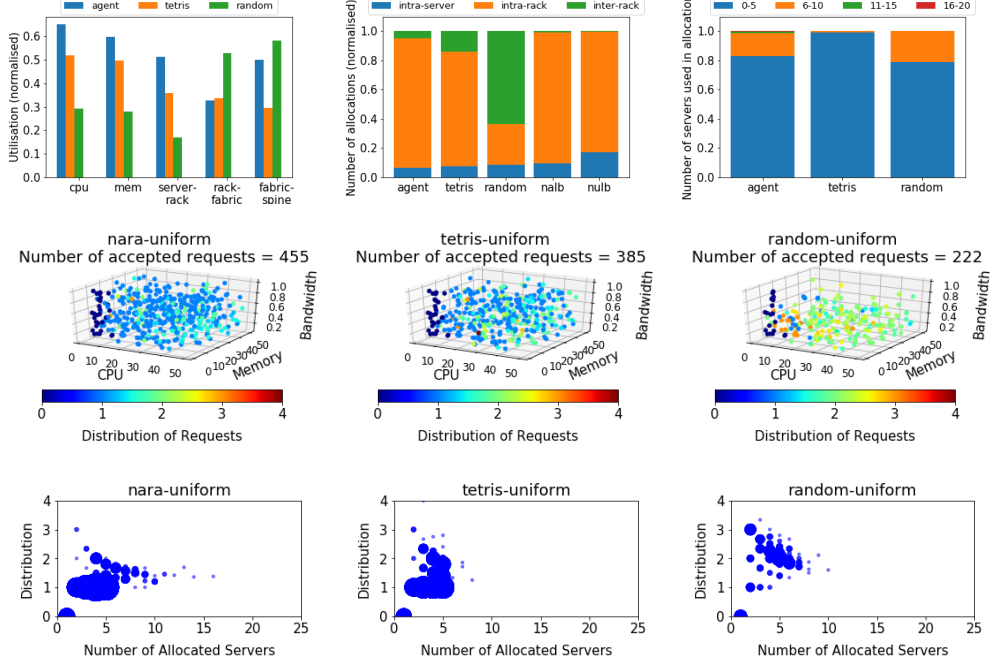


Figure 2: Top row: Bar plots comparing (left-right) resource utilisation (cpu, memory, bandwidth of tiers 1,2 and 3), allocation distribution characteristics and number of servers per allocation. Middle row: 3D plot representing the CPU, memory and bandwidth requirement per allocated request. Distribution value relates to how allocated server-nodes were spread throughout the data center where distribution of requests on single-node, intra-rack, inter-rack (neighbouring) and inter-rack (non-neighbouring) corresponds to heat map values of 0,1,2 and ≥ 3 . Bottom row: relationship between the number of servers allocated to a request, and their distribution throughout the DCN. Larger circles mean more requests with that value. Results from uniform on topology- α .

other. This metric does not, however, provide insight into the kind of requests being accepted, which is discussed in section 5.3. Resource utilisation, $(\frac{\text{Amount of resource } x \text{ used}}{\text{Amount of resource } x \text{ existing in DC}})$, indicates how much of the compute resources in the DC are idle. This is also a valuable metric since, as mentioned in section 1, idle servers still have significant energy requirements so high utilisation is desirable. Both values are continuous between 0 (worst) and 1 (best). All values for acceptance ratio and utilisation stated here and in the appendix have a 95% confidence interval of $\pm \leq 5\%$ of the stated value.

5.1 Basic performance

First, Nara was trained separately on each dataset (topology- α with 32 requests-per-episode) and compared against the baselines in the same scenario on 128-request episodes. Nara improves on acceptance ratio over the best performing baseline by 16%, 12% and 14% for the uniform, Azure and Alibaba datasets respectively. For utilisation, the improvement for (CPU,memory) is (10%,9%), (11%,12%) and (5%,4%) for the same three datasets respectively. Full results for acceptance ratio and utilisation on topology- α are shown in Table 1 and 2 (Appendix A) respectively.

Tetris is consistently the best performing baseline, though is still consistently worse than Nara. A qualitative and quantitative comparison of the two methods is discussed in section 5.3. It is also observed that the NULB method performs consistently worse than random on topology- α , but not on topology- β , which has more inter-rack bandwidth available between neighbouring racks. This is because the BFS based search method in NULB is bandwidth-agnostic. Because of this, given an initially chosen server to be allocated, it will perform a hops based search procedure through the graph that will systematically choose more servers to connect. If there is little inter-server bandwidth (as in topology- α), the method will have a high chance of systematically choosing a server for

Table 1: Acceptance ratio achieved by Nara and all 4 baselines across dataset-topology pairs. Nara is trained only on topology- α . Nara’s results for each dataset are those when trained on that dataset. NALB and NULB baselines were prohibitively slow on topologies larger than topology- α , and Tetris was prohibitively slow on topologies larger than topology- γ so these results are not shown. Best in bold.

Acceptance ratio												
Topology	Uniform				Azure				Alibaba			
	α	β	γ	δ	α	β	γ	δ	α	β	γ	δ
Nara	0.71	0.68	0.84	0.81	0.86	0.82	0.89	0.88	0.72	0.67	0.75	0.68
Tetris	0.61	0.6	0.63	-	0.77	0.67	0.71	-	0.63	0.6	0.7	-
NALB	0.52	0.45	-	-	0.68	0.65	-	-	0.44	0.43	-	-
NULB	0.29	0.42	-	-	0.5	0.53	-	-	0.2	0.44	-	-
Random	0.35	0.37	0.2	-	0.5	0.5	0.36	-	0.29	0.31	0.14	-
Agent improvement												
Best	16%	13%	33%	-	12%	22%	25%	-	14%	17%	7%	-
Random	102%	83%	302%	-	72%	64%	147%	-	148%	116%	436%	-

which no sufficiently provisioned path exists. In the other case, where inter-rack bandwidth is high, there is a much greater chance that, given a first choice of server, another can be found for which a sufficiently provisioned path exists. This observation also highlights an undesirable trait of hand-built heuristics, namely that one cannot always be confident that the heuristic’s desirable features will have a consistently positive effect (i.e. NULB’s strict locality adherence is only better than random in some cases). RL based methods such as Nara, on the other hand, do not presume any particular behaviours and are able to learn good solutions from exposure to problem instances on a case-by-case basis.

5.2 Generalisability

Differently shaped topologies. Two Nara agents, Agent- α and Agent- β , are trained on topology- α and β respectively, before being rolled out on topology- β (under the same train and test settings as in section 5.1). Agent- α was within 5% of Agent- β across all metrics on all datasets. Table 6 (Appendix B) show full numerical results for this test. Agent- α also maintains better performance on topology- β than all the baselines on each dataset. For acceptance ratio it maintains an improvement margin over the best baseline of 13%, 22% and 17% on the uniform, Azure and Alibaba datasets respectively. For (CPU,memory) utilisation the improvements were (15%,22%), (9%,18%) and (5%,5%) for the same datasets respectively. These results suggest that Nara learns a policy that is robust against changes in the network structure of the DCN. Full results shown in Appendix B.

Differently sized topologies. When trained on topology- α (32 requests-per-episode) and rolled out on topology- γ (896 requests-per-episode), Nara improves over Tetris by 33%, 25% and 7% for the uniform, Azure and Alibaba datasets respectively. Due to their recursive nature, NALB and NULB were prohibitively slow on the larger topologies so are not tested. Nara also maintains it’s policy on topology- δ (2048 requests-per-episode). Acceptance ratio is 14% better, 2% better and 6% worse for the uniform, Azure and Alibaba datasets compared to performance on topology- α . Resource utilisation values are higher for uniform and Azure, and 4% lower on Alibaba in the worst case. Full results shown in Appendix B.

Different request distributions. Three Nara agents were trained separately on each dataset. Each agent was then tested on the other two datasets (with the same training and test scenario as in section 5.1). The best-worst case performance degradation across all cross-dataset runs were 7%-11% for acceptance ratio, 2%-6% for CPU utilisation and 0%-15% for memory utilisation. Moreover, in each scenario all agents outperformed Tetris on each dataset. Full results shown in Appendix B.

5.3 Interpreting the policy

Here we observe the behaviour of Nara when tested on topology- α with uniform requests. The same plots for the other distributions are shown in Appendix C, from which the same behaviour described in this section can be observed. The top row in Fig. 2 shows that Nara keeps 88% of requests rack-local, uses 51% of rack-local (server-rack) bandwidth, and has 55% higher rack-local bandwidth utilisation than it does bandwidth between neighbouring racks (rack-fabric). Tetris, by comparison, has values of 78%, 36% and 6% for these features respectively. This indicates that Nara operates with a general preference for locality (rack and neighbouring racks).

The middle row of images shows that the majority of requests that Nara distributes widely (mostly across neighbouring racks) are those which have large CPU and memory requirements (therefore requiring a larger number of servers), but small ($\leq 50\%$ of maximum) bandwidth requirements. Nara uses the less bandwidth-dense rack-fabric network region (neighbouring racks) for requests requiring a large number of servers but a small amount of bandwidth provisioned along the paths inter-connecting these servers. This preserves the most bandwidth-dense region of the network (intra-rack) for the largest requests as well as the many smaller requests. Nara also tends to spread requests over a larger number of servers (17% spread over more than 5 servers, vs. Tetris' 1%). Fig. 2 also shows that requests that Nara spreads over the largest number of servers are also distributed mostly within a single rack (distribution ≤ 1.5), indicating that Nara will actively spread large (CPU-, memory- and bandwidth- heavy) requests over a large number of servers in the same rack (most servers have only partial resource availability due to allocations made to many smaller requests), keeping the allocation as rack-local as possible and exploiting this more bandwidth dense region despite.

From this we conclude about Nara:

1. *Locality is generally preferred*
2. *Requests that are CPU- and memory- heavy but bandwidth light, are spread across neighbouring racks; intra-rack bandwidth is preserved.*
3. *Requests that are both CPU-, memory- and bandwidth- heavy are spread over a large number of servers mostly within the same rack; preservation of the bandwidth dense intra-rack network is exploited for the largest requests imposing the greatest strain on the network.*

6 Limitations and future work

More substantial variation of DCN topology (scale, oversubscription structure) and request distribution (larger boundaries, more complex distribution shapes, non-homogeneous in the resource domain) would reveal a better evaluation of Nara's generalisability. Extending Nara to handle more complex requests built from sub-tasks with a dependency structure (similar to the work done in [22]) and/or incorporating latency alongside bandwidth into the DCN and the request requirements (e.g. requests might have a runtime that is determined by how much bandwidth and latency exists between inter-connected servers for example as in [18]) would see this work applied in an increasingly realistic DC environment, developing it's scope for application in the real world. Our network model simplifies away packet granularity of inter-server communication, and any associated queuing mechanism at the switches, which can in reality effect inter-server communication time and therefore request runtime. We intend to explore these natural extensions of this work in future iterations of it. Additionally, different reward structures (i.e. differently sized reward for successful and unsuccessful allocations or rewards based on different quantities) should be explored to ensure that the policy is being guided as best as possible during training.

7 Conclusion

We present Nara, a RL based framework that learns to solve the network-aware resource allocation problem for DCs. Using a GNN to produce graph embeddings representing the servers in the DC (the possible actions), trained end-to-end with a policy network that learns to make decision based on these representations and high level information about the DC, Nara is able to allocate more requests than previous hand-build heuristics, and demonstrates generalisability across different DCN topologies, scales and request distributions.

References

- [1] computerworld.com, “Why data centres are the new frontier in the fight against climate change.”
- [2] J. R. David Reinsel, John Gantz, “Data age 2025: The evolution of data to life-critical,” IDC Whitepaper, 2017.
- [3] buildings.com, “10 ways to save energy in your data center.”
- [4] Siemens, “Avoiding the five bottlenecks of data center planning and management,” 2019.
- [5] G. Porter, R. Strong, N. Farrington, A. Forencich, P. Chen-Sun, T. Rosing, Y. Fainman, G. Papen, and A. Vahdat, “Integrating microsecond circuit switching into the data center,” in *Proceedings of the ACM SIGCOMM 2013 Conference on SIGCOMM*, SIGCOMM ’13, (New York, NY, USA), p. 447–458, Association for Computing Machinery, 2013.
- [6] buildings.com, “Business technographics infrastructure survey, 2020.”
- [7] networkworld.com, “Top enterprise data center trends you need to know.”
- [8] networkworld.com, “Ethernet innovation pits power against speed.”
- [9] K. Bergman, “Empowering flexible and scalable high performance architectures with embedded photonics,” in *2018 IEEE International Parallel and Distributed Processing Symposium (IPDPS)*, pp. 378–378, 2018.
- [10] M. Isard, V. Prabhakaran, J. Currey, U. Wieder, K. Talwar, and A. Goldberg, “Quincy: Fair scheduling for distributed computing clusters,” in *Proceedings of the ACM SIGOPS 22nd Symposium on Operating Systems Principles, SOSP ’09*, (New York, NY, USA), p. 261–276, Association for Computing Machinery, 2009.
- [11] O. Hadary, L. Marshall, I. Menache, A. Pan, E. E. Greeff, D. Dion, S. Dorminey, S. Joshi, Y. Chen, M. Russinovich, and T. Moscibroda, “Protean: VM allocation service at scale,” in *14th USENIX Symposium on Operating Systems Design and Implementation (OSDI 20)*, pp. 845–861, USENIX Association, Nov. 2020.
- [12] A. Verma, L. Pedrosa, M. R. Korupolu, D. Oppenheimer, E. Tune, and J. Wilkes, “Large-scale cluster management at google with borg,” in *Proceedings of the European Conference on Computer Systems (EuroSys)*, (Bordeaux, France), 2015.
- [13] Facebook, *Engineering Blog Post: Introducing data center fabric, the next-generation Facebook data center network*, 2014.
- [14] X. Meng, V. Pappas, and L. Zhang, “Improving the scalability of data center networks with traffic-aware virtual machine placement,” in *2010 Proceedings IEEE INFOCOM*, pp. 1–9, 2010.
- [15] K. You, B. Tang, and F. Ding, “Near-optimal virtual machine placement with product traffic pattern in data centers,” in *2013 IEEE International Conference on Communications (ICC)*, pp. 3705–3709, 2013.
- [16] G. Koslovski, S. Soudan, P. Gonçalves, and P. Vicat-Blanc, “Locating virtual infrastructures: Users and inp perspectives,” in *12th IFIP/IEEE International Symposium on Integrated Network Management (IM 2011) and Workshops*, pp. 153–160, 2011.
- [17] M. G. Rabbani, R. P. Esteves, M. Podlesny, G. Simon, L. Z. Granville, and R. Boutaba, “On tackling virtual data center embedding problem,” in *2013 IFIP/IEEE International Symposium on Integrated Network Management (IM 2013)*, pp. 177–184, 2013.
- [18] G. Zervas, H. Yuan, A. Saljoghei, Q. Chen, and V. Mishra, “Optically disaggregated data centers with minimal remote memory latency: Technologies, architectures, and resource allocation,” *J. Opt. Commun. Netw.*, vol. 10, pp. A270–A285, Feb 2018.
- [19] R. Grandl, G. Ananthanarayanan, S. Kandula, S. Rao, and A. Akella, “Multi-resource packing for cluster schedulers,” *SIGCOMM Comput. Commun. Rev.*, vol. 44, p. 455–466, Aug. 2014.
- [20] E. Khalil, H. Dai, Y. Zhang, B. Dilkina, and L. Song, “Learning combinatorial optimization algorithms over graphs,” in *Advances in Neural Information Processing Systems 30* (I. Guyon, U. V. Luxburg, S. Bengio, H. Wallach, R. Fergus, S. Vishwanathan, and R. Garnett, eds.), pp. 6348–6358, Curran Associates, Inc., 2017.

- [21] S. Manchanda, A. MITTAL, A. Dhawan, S. Medya, S. Ranu, and A. Singh, “Gcomb: Learning budget-constrained combinatorial algorithms over billion-sized graphs,” in *Advances in Neural Information Processing Systems* (H. Larochelle, M. Ranzato, R. Hadsell, M. F. Balcan, and H. Lin, eds.), vol. 33, pp. 20000–20011, Curran Associates, Inc., 2020.
- [22] H. Mao, M. Schwarzkopf, S. B. Venkatakrisnan, Z. Meng, and M. Alizadeh, “Learning scheduling algorithms for data processing clusters,” in *Proceedings of the ACM Special Interest Group on Data Communication, SIGCOMM ’19*, (New York, NY, USA), p. 270–288, Association for Computing Machinery, 2019.
- [23] A. Mirhoseini, H. Pham, Q. V. Le, B. Steiner, R. Larsen, Y. Zhou, N. Kumar, M. Norouzi, S. Bengio, and J. Dean, “Device placement optimization with reinforcement learning,” in *International Conference on Machine Learning*, pp. 2430–2439, PMLR, 2017.
- [24] R. Addanki, S. B. Venkatakrisnan, S. Gupta, H. Mao, and M. Alizadeh, “Placeto: Learning generalizable device placement algorithms for distributed machine learning,” *arXiv preprint arXiv:1906.08879*, 2019.
- [25] A. Paliwal, F. Gimeno, V. Nair, Y. Li, M. Lubin, P. Kohli, and O. Vinyals, “Reinforced genetic algorithm learning for optimizing computation graphs,” in *International Conference on Learning Representations*, 2020.
- [26] J. Suárez-Varela, A. Mestres, J. Yu, L. Kuang, H. Feng, P. Barlet-Ros, and A. Cabellos-Aparicio, “Routing based on deep reinforcement learning in optical transport networks,” in *2019 Optical Fiber Communications Conference and Exhibition (OFC)*, pp. 1–3, 2019.
- [27] K. Rusek, J. Suárez-Varela, P. Almasan, P. Barlet-Ros, and A. Cabellos-Aparicio, “Routenet: Leveraging graph neural networks for network modeling and optimization in sdn,” *IEEE Journal on Selected Areas in Communications*, vol. 38, no. 10, pp. 2260–2270, 2020.
- [28] Z. Yan, J. Ge, Y. Wu, L. Li, and T. Li, “Automatic virtual network embedding: A deep reinforcement learning approach with graph convolutional networks,” *IEEE Journal on Selected Areas in Communications*, vol. 38, no. 6, pp. 1040–1057, 2020.
- [29] I. Drori, A. Kharkar, W. R. Sickinger, B. Kates, Q. Ma, S. Ge, E. Dolev, B. Dietrich, D. P. Williamson, and M. Udell, “Learning to solve combinatorial optimization problems on real-world graphs in linear time,” in *2020 19th IEEE International Conference on Machine Learning and Applications (ICMLA)*, pp. 19–24, 2020.
- [30] J. Schulman, F. Wolski, P. Dhariwal, A. Radford, and O. Klimov, “Proximal policy optimization algorithms,” *CoRR*, vol. abs/1707.06347, 2017.
- [31] W. Hamilton, Z. Ying, and J. Leskovec, “Inductive representation learning on large graphs,” in *Advances in Neural Information Processing Systems* (I. Guyon, U. V. Luxburg, S. Bengio, H. Wallach, R. Fergus, S. Vishwanathan, and R. Garnett, eds.), vol. 30, Curran Associates, Inc., 2017.
- [32] Alibaba, *Alibaba Cluster Trace Program*, 2018.
- [33] M. Wang, D. Zheng, Z. Ye, Q. Gan, M. Li, X. Song, J. Zhou, C. Ma, L. Yu, Y. Gai, T. Xiao, T. He, G. Karypis, J. Li, and Z. Zhang, “Deep graph library: A graph-centric, highly-performant package for graph neural networks,” *arXiv preprint arXiv:1909.01315*, 2019.
- [34] G. Brockman, V. Cheung, L. Pettersson, J. Schneider, J. Schulman, J. Tang, and W. Zaremba, “Openai gym,” 2016. cite arxiv:1606.01540.
- [35] E. Liang, R. Liaw, R. Nishihara, P. Moritz, R. Fox, J. Gonzalez, K. Goldberg, and I. Stoica, “Ray rllib: A composable and scalable reinforcement learning library,” *CoRR*, vol. abs/1712.09381, 2017.
- [36] M. Abadi, A. Agarwal, P. Barham, E. Brevdo, Z. Chen, C. Citro, G. S. Corrado, A. Davis, J. Dean, M. Devin, S. Ghemawat, I. Goodfellow, A. Harp, G. Irving, M. Isard, Y. Jia, R. Jozefowicz, L. Kaiser, M. Kudlur, J. Levenberg, D. Mané, R. Monga, S. Moore, D. Murray, C. Olah, M. Schuster, J. Shlens, B. Steiner, I. Sutskever, K. Talwar, P. Tucker, V. Vanhoucke, V. Vasudevan, F. Viégas, O. Vinyals, P. Warden, M. Wattenberg, M. Wicke, Y. Yu, and X. Zheng, “TensorFlow: Large-scale machine learning on heterogeneous systems,” 2015. Software available from tensorflow.org.

A Utilisation data for other topologies

Tables 2, 3, 4 and 5 show the full numerical results for the utilisation values (CPU and memory) for Nara on topology- α , β , γ and δ respectively.

Table 2: Resource utilisation of all three resource domains after convergence with 128 requests averaged over 5 distinct rollouts on the three datasets for the DCN topology referred to as α in Table 8. Best in bold.

Resource utilisation on topology- α						
Resource	Uniform		Azure		Alibaba	
	CPU	Memory	CPU	Memory	CPU	Memory
Nara [This work]	0.64	0.62	0.62	0.47	0.81	0.24
Tetris [19]	0.58	0.57	0.56	0.42	0.77	0.23
NALB [18]	0.47	0.46	0.43	0.31	0.6	0.18
NULB [18]	0.23	0.23	0.32	0.28	0.27	0.08
Random	0.3	0.31	0.38	0.26	0.42	0.12
Nara improvement						
Best baseline	10%	9%	11%	12%	5%	4%
Random	113%	100%	63%	81%	93%	100%

Table 3: Resource utilisation of all three resource domains after convergence with 128 requests averaged over 5 distinct rollouts the three datasets for the DCN topology referred to as β in Table 8. Best in bold.

Resource utilisation on topology- β						
Resource	Uniform		Azure		Alibaba	
	CPU	Memory	CPU	Memory	CPU	Memory
Nara [This work]	0.62	0.62	0.62	0.47	0.79	0.23
Tetris [19]	0.54	0.51	0.57	0.4	0.75	0.22
NALB [18]	0.36	0.36	0.48	0.32	0.55	0.15
NULB [18]	0.34	0.31	0.4	0.32	0.5	0.15
Random	0.29	0.27	0.43	0.27	0.44	0.13
Nara improvement						
Best baseline	15%	22%	9%	18%	5%	5%
Random	114%	130%	35%	56%	80%	77%

B Cross- topology and dataset results

Tables 6 and 7 show the full numerical results for the cross-topology and cross-dataset results described in Section 5.2.

C Interpretation of Nara’s policy on other graphs and datasets

Figures 3, 4 and 5 show the same visualisations shown in section 5.3, but for Nara and all baselines. Fig. 6 shows the histogram, and overlaid probability density plots of the distribution of allocated requests for the same set of rollouts.

Figs. 7 shows the relationship between request size and distribution, the relationship between the number of servers allocated and distribution and a histogram detailing the distribution of all allocated

Table 4: Resource utilisation of all three resource domains after convergence with 896 requests averaged over 5 distinct rollouts on the three datasets for the DCN topology referred to as γ in Table 8. Best in bold.

Resource utilisation on topology- γ						
Resource	Uniform		Azure		Alibaba	
	CPU	Memory	CPU	Memory	CPU	Memory
Nara [This work]	0.74	0.75	0.71	0.53	0.87	0.25
Tetris [19]	0.52	0.5	0.53	0.39	0.83	0.25
Random	0.15	0.13	0.18	0.13	0.16	0.05
Nara improvement						
Best baseline	37%	50%	34%	36%	5%	0%
Random	393%	476%	294%	308%	444%	400%

Table 5: Resource utilisation of all three resource domains after convergence with 4096 requests averaged over 5 distinct rollouts on the three datasets for the DCN topology referred to as δ in Table 8. Best in bold.

Resource utilisation on topology- δ						
Resource	Uniform		Azure		Alibaba	
	CPU	Memory	CPU	Memory	CPU	Memory
Nara [This work]	0.74	0.75	0.72	0.51	0.79	0.23

requests for Nara trained and rolled out on the uniform, Azure and Alibaba datasets. Fig. 8 shows the same analysis as in Fig. 2 (middle row) comparing Nara (agent), Tetris and random on the Azure and Alibaba datasets. Following from what is observed and discussed in section 5.3, the same patterns are seen in these images, suggesting as stated in section 5.3 that the policies learnt by Nara on each dataset separately have similar high level traits as detailed at the end of section 5.3.

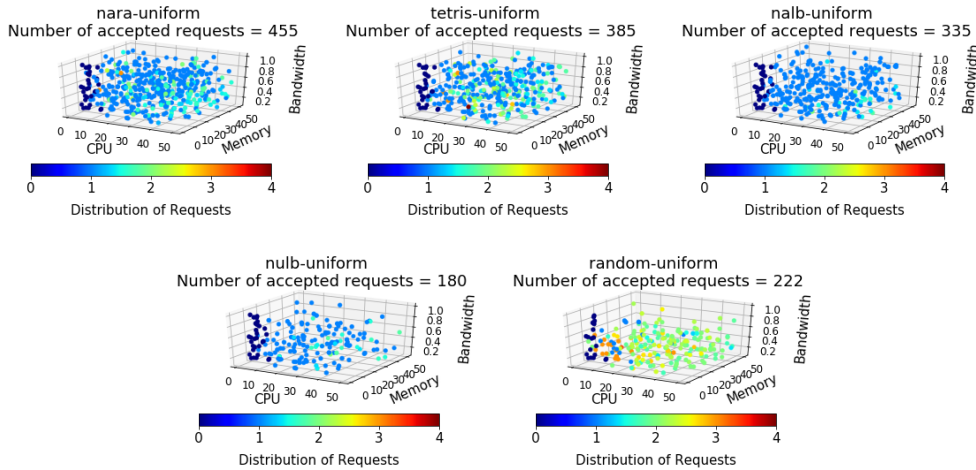


Figure 3: Same visualisation as in Fig 2 for (left-right, top-bottom) Nara, Tetris NALB, NULB and random heuristics with the uniform request dataset and topology- α .

Table 6: Comparison of acceptance ratio (‘Accpt.’), CPU and Memory utilisation (‘CPU’, ‘Mem.’) achieved by 2 distinct Nara agents. Agent- α is trained on topology- α and then rolled out on topology- β and Agent- β is trained and rolled out on topology β .

Cross-topology performance comparison on topology- β									
Metric	Uniform			Azure			Alibaba		
	Accpt.	CPU	Mem.	Accpt.	CPU	Mem.	Accpt.	CPU	Mem.
Agent- α	0.68	0.62	0.62	0.82	0.62	0.47	0.67	0.79	0.23
Agent- β	0.70	0.64	0.61	0.82	0.6	0.46	0.68	0.8	0.24

Table 7: Comparison of acceptance ratio (‘Accpt.’), CPU and Memory utilisation (‘CPU’, ‘Mem.’) achieved by 3 different Nara agents each trained on a specific dataset and then rolled out on the other two. Underlined values are the values achieved by an agent on the dataset it saw during training. Results from the Tetris baseline included for reference.

Cross-dataset performance comparison									
Metric	Uniform			Azure			Alibaba		
	Accpt.	CPU	Mem.	Accpt.	CPU	Mem.	Accpt.	CPU	Mem.
Agent-uniform	<u>0.71</u>	<u>0.64</u>	<u>0.62</u>	0.83	0.6	0.48	0.64	0.79	0.24
Agent-Azure	0.71	0.65	0.62	<u>0.86</u>	<u>0.62</u>	<u>0.47</u>	0.68	0.81	0.24
Agent-Alibaba	0.66	0.61	0.59	0.77	0.58	0.41	<u>0.72</u>	<u>0.81</u>	<u>0.24</u>
Tetris	0.61	0.58	0.57	0.83	0.56	0.41	0.63	0.77	0.23

D Baseline implementations

D.1 Tetris

Tetris encourages locality, and thus reduces network congestion, by penalising the use of remote resources. In its original conception this was applied largely in the context of remote storage resources. In our simplified DCN scenario we have homogeneous servers, and so apply the penalty to rack-non-local server-nodes in the DCN, given the first node chosen to be allocated to a particular request, so as to employ this penalty system in the homogenous case.

Penalty values were tested between 10% and 100% in increments of 10%, concluding an optimal value of 90%.

D.2 Network (un)aware locality based

The NALB and NULB use a length and bandwidth weighted k-shortest path routing procedure, as they are designed to be able to balance both bandwidth provisions and latency of communication. However, in our implementation we do not account for latency since no notion of distance or communication speed is accounted for in our DCN scenario, so we implement k-shortest path routing with bandwidth weighting only.

E Model details

E.1 Action representation model

Each NN associated with the message passing stage i , W_i , has an output dimension of 16 units. The size of the input vector (i.e. the raw feature vector of the DCN server-nodes) to the first aggregation layer, W_0 , has dimension of 8 ($[cpu, memory, bandwidth, selected]$) where *selected* is a binary

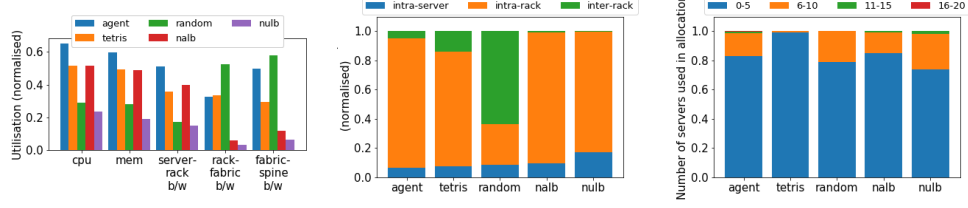


Figure 4: Same visualisation as in Fig 2 for Nara (agent) and all baselines.

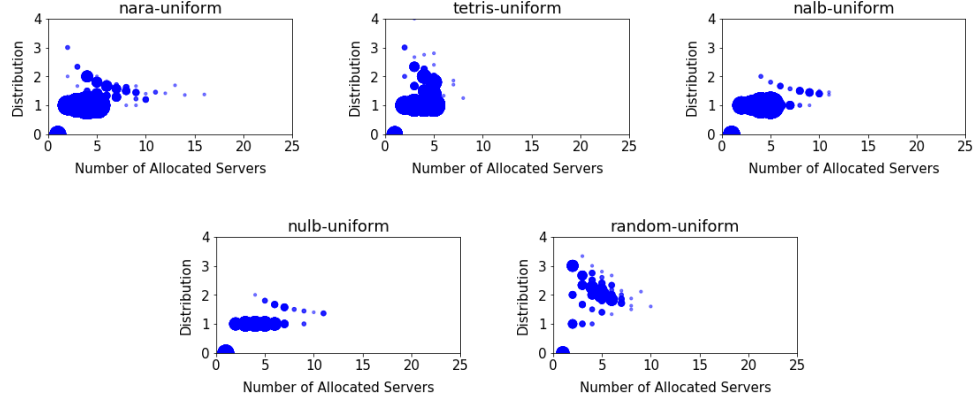


Figure 5: Same visualisation as in Fig 2 for (left-right, top-bottom) Nara, Tetris NALB, NULB and random heuristics with the uniform request dataset and topology- α .

indicator specifying if that node is allocated to the current request. Relu activations are used for each aggregation layer.

Three message passing stages (and therefore 3 NNs) were used. This is chosen so that information about the full local network state can be received by each server-node (i.e. the state of its directly connected server-rack, rack-fabric and fabric-spine switches links).

Embedding size was determined by grid search over the values [4, 8, 16].

E.2 Policy model

The first NN P_1 outputs an 8 dimensional representation of the observation vector and has an 8 dimensional hidden layer.

The second, P_2 , has a single layer which outputs a 1 dimensional value (i.e. the logit for each action). The input dimension is the size of the action representation dimension + observation representation dimension (i.e. $16 + 8 = 24$ in our specific configuration).

The size of the hidden layer and final output size were determined by grid search over the values [4, 8, 16].

E.3 Training and Implementation details

All models were trained with a single Nvidia V100 GPU on a university hosted cluster with Intel(R) Xeon(R) Gold 6148 CPUs.

The GNN model was written using the Deep Graph Library (DGL, Apache License) [33]. The DCN RL environment was written using OpenAI Gym (MIT License) [34] and the Ray RLlib [35] (Apache License) library’s implementation of the PPO algorithm [30] was used for training. Both DGL and RLlib were used with a Tensorflow 2 (Apache License) [36] backend.

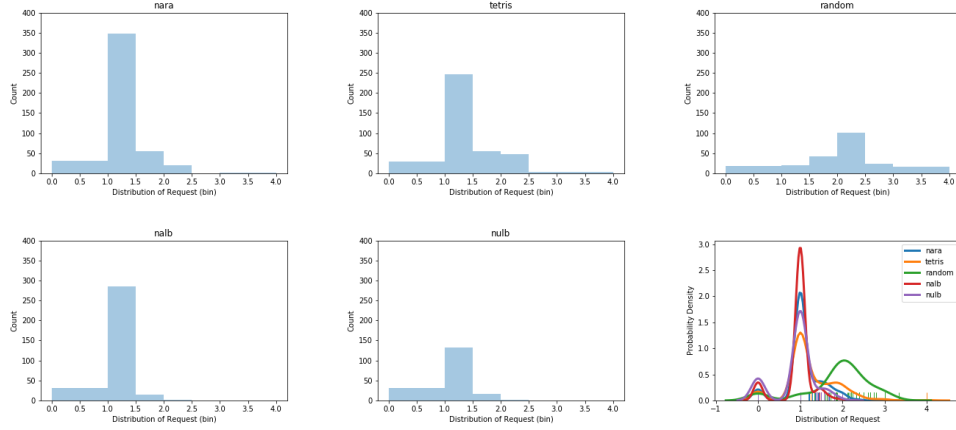


Figure 6: Histograms and a probability density plot (bottom right image) of the distribution of successfully allocated requests for Nara and all baselines. Distribution values are the same as described in the caption of Fig. 2. Results are for uniform request on topology- α .

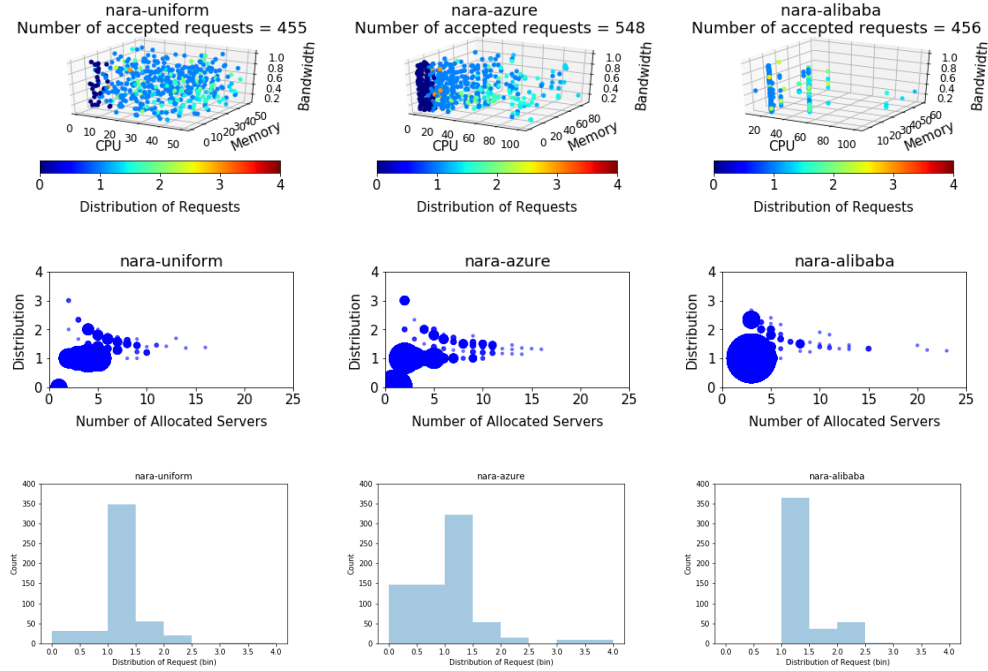


Figure 7: Request-distribution (top row) and servers-distribution (second row) plots are the same as described in the caption of Fig. 2. Bottom row are histograms showing how many requests are allocated with what distribution. Left-right is uniform-agent, Azure-agent, Alibaba-agent (for both rows). Results are for topology- α .

Nara was trained with a learning rate of 5×10^{-3} , with (according to the naming convention of variables used by RLlib) `train_batch_size = 2048`, `sgd_minibatch_size = 256`, `batch_mode = complete_episodes`, `vf_share_layers = False` and `eager_tracing = True`. Default parameters were used otherwise.

`train_batch_size`, `sgd_minibatch_size` and `learning_rate` were chosen by a simple grid search over the values `[512, 1024, 2056]`, `[32, 64, 128, 256]` and `[5×10^{-3} , 5×10^{-4} , 5×10^{-5}]` respectively.

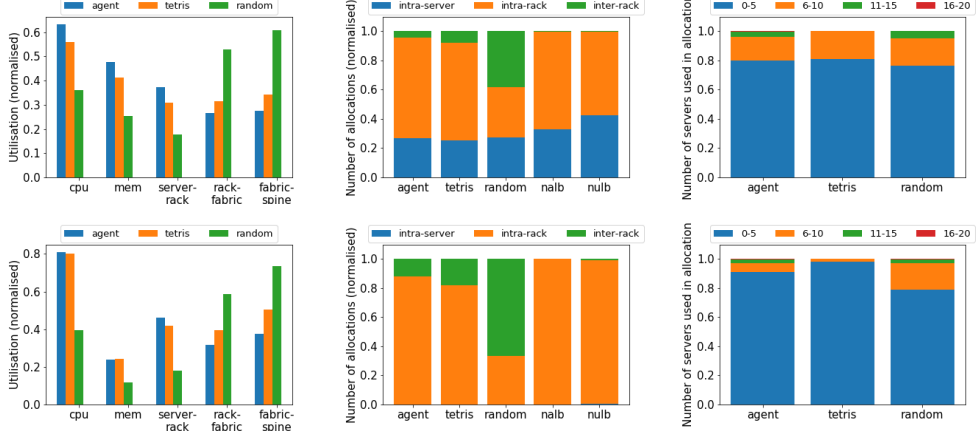


Figure 8: Same visualisation as in Fig 4 for Nara (agent) and all baseline on the Azure (top) and Alibaba (bottom) datasets.

Nara was trained on episode lengths of 32 (i.e. it would attempt to serve 32 requests one-by-one before episode termination). Nara was trained over 150 training iterations with the aforementioned training parameters per-iteration. Nara could train to convergence in under 3 hours (approximately 150,000 training steps) given the training parameters and available compute resources.

Values for the reward components (x , y , z) defined in section 3.2 were determined by trial and error over multiple combinations, where values of x and y within the set $\{\pm 100, \pm 50, \pm 10, \pm 1\}$ and values of z within the set $\{-1, -10, 0\}$.

F Topologies

Fig 9 shows the DCN topologies of topology- α , β and γ . Larger DCN graphs are not shown as they have too many nodes to be clearly plotted. Table 8 details high level information about the topologies used in this work.

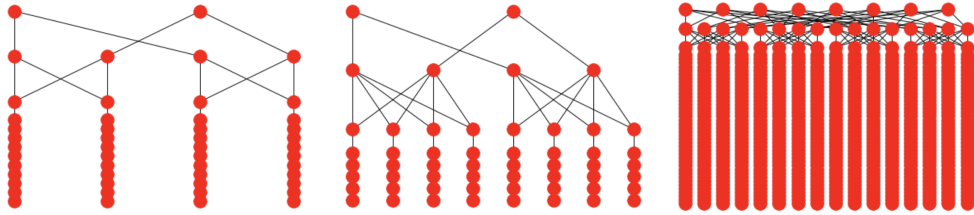


Figure 9: Left to right: topology- α , topology- β , topology- γ . Vertically aligned clusters of nodes that are very close together represent the compute/memory nodes in a rack.

G DCN environment

Each server has 10 units of CPU and 10 units of memory (both discrete). In topologies- α and β links in all network tiers had 1 continuous unit of bandwidth. In larger topologies, links in the rack-fabric and fabric-spine tiers had 2 continuous units of bandwidth.

The simulation does not account for a notion of time-domain management (e.g. given a set of requests that arrive simultaneously, determine in what order they will be served). This was a design choice done in order to isolate the compute + network packing aspect of resource management. Indeed, in real DCNs requests arrive stochastically, and some time-domain management has to be implemented. However, the goal of this work is to demonstrate a framework that is able to maximise the probability of finding a valid packing for a request, given a particular state of the DCN. In effect, the simulation

Table 8: Characteristics of DCN topologies used in the experiment.

DCN Topology Characteristics				
Topology	α	β	γ	δ
Train	✓	×	×	×
Test	✓	✓	✓	✓
Server per Rack	10	5	40	40
Number of Racks	4	8	16	64
Number of Servers	40	40	640	2560
Rack-fabric oversubscription	2:1	4:1	2:1	2:1
Server-rack oversubscription	5:1	5:2	5:1	5:1

operates a first-in-first-out (FIFO) buffer with a size of 1, where failed requests are dropped and replaced by the next arrival. For the same reason, a notion of priority is not included in the request structure - all allocated requests will retain access to their resources until their holding period has expired. In the future, a system which is able to make resource management decisions in both the resource- and time- domain may be explored. In this work, however, we seek to demonstrate only the former, to which scalable reinforcement learning methods have not yet been applied.

When the allocating entity (RL based or otherwise) chooses another node from which resources will be allocated to some request, the simulation environment will undergo a k-shortest paths route finding procedure. If paths can be found (subject to the constraints defined in section 3.1) then the node is accepted into the solution set and the allocation procedure continues. If a path cannot be found for some pair of nodes within the currently proposed solution set (including the most recently selected one for which paths are being checked), then this will constitute a failed allocation. $K = 3$ in all experiments.

H Datasets

The Alibaba [32] and Azure [11] datasets were split into test and train subsets of 80% and 20% respectively.

We define the ‘average load’ in this context as the average maximum amount of resource being requested/used in a given moment (i.e. if every request was successfully allocated, what would be the average resource demand on the DCN in a given moment, accounting for both currently allocated requests and the awaiting request). The bounds of the uniform distribution for the holding period and the episode length (number of requests seen before termination) each dataset were set to enforce an average load of 95%, 90% and 90% respectively. This ensures that trivial policies (e.g. random allocation) can not be mistaken for performing well, since if the average load is consistently very small, then there is typically very little strain on the compute and networking resources in the DCN and therefore the allocation constraints stated in 3.1 could be trivial to satisfy.

Figure 10 shows the distributions of the augmented cluster trace datasets. Random-uniform traffic was generated to accompany the (scaled) Azure and Alibaba CPU and memory requirements with a maximum requirements of 1 (i.e. the maximum possible provision by a single server-rack link).

For the Azure dataset, the compute and memory resources were scaled by $50\times$ and bound to not request more than 10 servers worth of resources in each server-resource domain (100 units).

For the Alibaba dataset, the compute and memory resources were scaled by $50\times$ and $5\times$ respectively and bound to not request more than 10 servers worth of resources in each server-resource domain (100 units).

For both uniform, Azure and Alibaba, the bandwidth were uniformly request, from 10% to 100% of the server-rack link bandwidth.

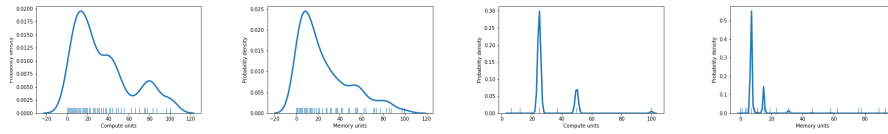


Figure 10: Left-right: probability density of request quantities for Azure-CPU, Azure-memory, Alibaba-CPU, Alibaba-memory. Each server in all topologies has 10 discrete CPU memory units and each server-rack link has 1 continuous bandwidth unit. Vertical lines along the x axis represent values that exist in the dataset.